DALTON
FULL PAPER

Reaction of $[Ni(Ph_2PCH_2CH_2PPh_2)_2]$ with DCl: controlling the formation of HD and D_2*

Sian C. Davies, Richard A. Henderson, David L. Hughes and Kay E. Oglieve

Nitrogen Fixation Laboratory, John Innes Centre, Norwich Research Park, Colney, Norwich, UK NR4 7UH

The reaction between anhydrous DCl and $[Ni(Ph_2PCH_2CH_2PPh_2)_2]$ in dichloromethane produced mixtures of HD and D_2. The relative amounts of the dihydrogen isotopomers produced depends on the concentration of acid. Mechanistic investigations showed that the reaction involves initial formation of $[NiD(Ph_2PCH_2CH_2PPh_2)_2]^+$. This deuteriation labilises the nickel to phosphine dissociation. At low concentrations of acid, phosphine chelate ring opening produces $[NiCl_2(Ph_2PCH_2CH_2PPh_2)]$ (confirmed by X-ray crystallography) and free $Ph_2PCH_2CH_2PPh_2$ together with HD (65 ± 5) and D_2 (35 ± 5%). The hydrogen atom of HD originates from a phosphine ligand. At high concentrations of acid the rate of attack of DCl at $[NiD(Ph_2PCH_2CH_2PPh_2)_2]^+$ becomes faster than phosphine chelate ring opening and results in the formation of $[Ni(Ph_2PCH_2CH_2PPh_2)_2]Cl_2$ and predominantly D_2. Experimentally, the highest concentration of DCl that can be used without appreciable decomposition of the complex is 0.2 mol dm^{-3}. At this concentration of acid the dihydrogen isotopomer distribution is HD (35 ± 5) and D_2 (65 ± 5%); however, analysis of the product distribution indicates that at much higher acid concentrations D_2 could be the exclusive isotopomer.

The diprotonation of electron-rich metal sites, followed by intramolecular coupling of the two hydride ligands and subsequent release of dihydrogen [equation (1), where *M* represents

$$M \overset{H^+}{\rightleftharpoons} (M\text{–H})^+ \overset{H^+}{\rightleftharpoons} (\text{H}\text{–}M\text{–H})^{2+} \longrightarrow M^{2+} + H_2 \qquad (1)$$

the metal and its ancillary ligands], is a conceptually simple mechanism, which has been observed in many systems[1] and presumed in a great many others. In principle, this sequence of reactions could produce H_2, D_2 or HD selectively, depending on the acid used at each stage. However, this is as yet an unrealised goal, primarily because intra- and inter-molecular exchange reactions effectively destroy the selectivity.[2,3] For example, equation (1) indicates that the reaction with D^+ would produce only D_2. However, in many systems, the metal has ancillary ligands bound to it which contain hydrogen atoms. These hydrogens can undergo intramolecular exchange with the deuteride ligand (*e.g.* orthometallation), effectively scrambling deuterium and hydrogens between metal and ligand and resulting in a mixture of D_2, HD and H_2.

Equation (1) also suggests a pathway for forming HD selectively. In the first step the reaction of *M* with H^+ gives *M*–H^+. Isolation of this complex followed by reaction with D^+ could produce HD. However, again, intramolecular exchange between the deuteride ligand and hydrogen atoms on ancillary ligands results in scrambling of the deuterium between metal and ligand. In addition, rapid exchange of the initially formed *M*–H^+ with D^+ leads to a loss of selectivity.

Herein, we report kinetic and product analysis studies on the reaction between $[Ni(dppe)_2]$ (dppe = $Ph_2PCH_2CH_2PPh_2$) and anhydrous HCl or DCl (>90% D-labelled) in dichloromethane or tetrahydrofuran (thf). We show that the dihydrogen isotopomer products can be changed by simply varying the concentration of acid.

* *Supplementary data available*: first-order rate constants, isotopomer distribution. For direct electronic access see http://www.rsc.org/suppdata/dt/1998/425/, otherwise available from BLDSC (No. SUP 57327, 4 pp.) or the RSC Library. See Instructions for Authors, 1998, Issue 1 (http://www.rsc.org/dalton).

Experimental

Preparation of complexes

All manipulations were routinely performed under an atmosphere of dinitrogen, using Schlenk or syringe techniques as appropriate. All solvents were freshly distilled from the appropriate drying agents immediately prior to use; thf was distilled from sodium–benzophenone and dichloromethane from phosphorus pentaoxide.

The complexes used in this study, $[Ni(dppe)_2]$ and $[NiH(dppe)_2]BF_4$, were prepared by methods described in the literature.[4,5] The NMR and IR spectral data, together with elemental analyses of these complexes are shown in Table 1. IR spectra were recorded on a Perkin-Elmer 883 spectrophotometer, NMR spectra by use of either a JEOL GSX 270 MHz, or a Lambda 400 MHz spectrometer.

The product of the reaction between $[Ni(dppe)_2]$ and anhydrous HCl in thf is $[NiCl_2(dppe)]$, identified by X-ray crystallography (see below). Spectroscopic characterisation of this complex is shown in Table 1. The product of the same reaction in dichloromethane at high concentrations of acid is $[Ni(dppe)_2]^{2+}$, which was detected in solution by $^{31}P\text{-}\{^1H\}$ NMR spectroscopy. An authentic sample of $[Ni(dppe)_2][BF_4]_2$, prepared from the reaction of $[NiH(dppe)_2]BF_4$ with 5 equivalents of $HBF_4{\cdot}OEt_2$ in dichloromethane,[6] gave the same spectrum.

Crystallography

Crystal data for $[NiCl_2(dppe)]$. $C_{26}H_{24}Cl_2NiP_2$, $M = 528.0$, monoclinic, space group $P2_1/c$ (no. 14), $a = 11.4368(13)$, $b = 13.356(2)$, $c = 15.975(4)$ Å, $\beta = 99.10(2)°$, $U = 2409.6(7)$ Å^3, $Z = 4$, $D_c = 1.46$ g cm^{-3}, $F(000) = 1088$, $T = 293$ K, μ(Mo-Kα) = 11.7 cm^{-1}, λ(Mo-Kα) = 0.710 69 Å.

Crystals of the complex are reddish brown prisms. One was cut to *ca.* 0.48 × 0.24 × 0.19 mm and mounted on a glass fibre. After preliminary photographic examination this was then transferred to an Enraf-Nonius CAD4 diffractometer (with monochromated radiation) for determination of accurate cell parameters (from the settings of 25 reflections, $\theta = 10$–$11°$, each centred in four orientations) and for measurement of diffraction intensities (4232 unique reflections to $\theta_{max} = 25°$; 3377 were 'observed' with $I > 2\sigma_I$).

During processing, corrections were applied for Lorentz-polarisation effects, slight crystal deterioration, absorption (by semiempirical ψ-scan methods) and to remove negative net intensities (by Bayesian statistical methods). The structure was determined by the heavy-atom method using the SHELX 76 program[7] and refined, on F^2, by full-matrix least-squares methods, using SHELXL 93.[8] Hydrogen atoms were included in idealised positions but all parameters were allowed to refine freely. The non-hydrogen atoms were refined with anisotropic thermal parameters. At the conclusion of the refinement, $wR2 = 0.080$ and $R1 = 0.041$[8] for all data weighted $w = [\sigma^2(F_o^2) + (0.0341P)^2 + 0.69P]^{-1}$ with $P = (F_o^2 + 2F_c^2)/3$; for the 'observed' data only, $R1 = 0.030$. In the final difference map the highest peaks (to *ca.* 0.42 e Å^{-3}) were close to the Ni atom.

This structure is the same as that reported and described for the product of the reaction of dppe with $NiCl_2 \cdot 6H_2O$ in hot propan-2-ol–methanol;[9] we therefore record our (more precise) results here only briefly. Scattering factors for neutral atoms were taken from ref. 10. Computer programs used in this analysis have been noted above or in Table 4 of ref. 11, and were run on a DEC-AlphaStation 200 4/100. CCDC reference number 186/806.

Kinetic measurements

(1) Formation of $[NiH(dppe)_2]^+$. The kinetics of the reaction between $[Ni(dppe)_2]$ and anhydrous HCl in thf, were measured using a Hi-Tech SF-51 stopped-flow spectrophotometer, modified to handle air-sensitive materials.[12] The temperature was maintained at 25.0 ± 0.1 °C using a Grant LE8 thermostat tank. The spectrophotometer is interfaced to a Viglen computer *via* an analogue to digital converter. The kinetics were followed by monitoring the absorbance changes associated with the nickel complex, in the range λ = 400–480 nm (<450 nm, absorbance decrease; >450 nm, absorbance increase). The data reported in this paper are those collected at λ = 420 nm and a typical absorbance *vs*. time curve is shown in Fig. 2. The observed rate constants were independent of the wavelength used to study the reaction.

Solutions of anhydrous HCl (100 mmol dm^{-3}) were prepared by mixing MeOH (0.1 cm^3) and $SiMe_3Cl$ (0.32 cm^3) in thf (25 cm^3). More dilute solutions were prepared from this stock. All solutions were used within 1 h of preparation to minimise acid-catalysed decomposition of the solvent. The ionic strength of the solutions was kept constant at $I = 0.1$ mol dm^{-3} using $[NBu^n_4]BF_4$.

The reactions were studied under pseudo-first-order conditions {[HCl] ≥ 10[Ni(dppe)$_2$]}. The traces were an excellent fit to a single exponential for greater than three half-lives. The observed rate constants (k_{obs}) were determined by a curve-fitting computer program.

(2) Release of dihydrogen. Gas chromatographic dihydrogen analyses were performed on a Phillips PU 4400 gas chromatograph with a thermal conductivity detector. Separation was on an alumina column using argon as the carrier gas, at an operating temperature of 60 °C. In a typical analysis, $[Ni(dppe)_2]$ (0.04 g, 0.047 mmol) was weighed into a one-necked flask (50 cm^3) together with a stirrer-bar. The flask was sealed with a rubber septum, evacuated and purged with dinitrogen *via* a needle connector. In a separate Schlenk flask, a stock solution of anhydrous HCl (100 mmol dm^{-3}) was prepared, and then degassed. A sample (10 cm^3) of this solution was drawn into an air-tight syringe and rapidly injected through the septum onto the $[Ni(dppe)_2]$.

For kinetic experiments, stirring and timing commenced on injection of the acid. At appropriate time intervals, samples (0.1 cm^3) of the gas mixture were taken into a gas-tight syringe and analysed by GC. For each sample analysed, the peak areas (P) from the chromatographs are directly proportional to the concentration of dihydrogen. The kinetics of dihydrogen production were analysed by the usual semilogarithmic plot of $\log_e(P_t - P_\infty)$ against time t (where P_t is the peak area at time t and P_∞ that when the reaction is complete). The gradient of the resulting straight line is the observed rate constant.[13]

Table 1 Analytical and spectroscopic characterisation of the complexes[a]

	Elemental analysis[b] (%)		
Complex	C	H	^{31}P-{^{1}H}[c]
$[Ni(dppe)_2]$	73.3 (73.0)	5.6 (5.6)	−99.1
$[NiH(dppe)_2]BF_4$[d]	66.1 (66.2)	5.1 (5.2)	−97.7
$[Ni(dppe)_2][BF_4]_2$	58.3 (58.3)	4.6 (4.7)	−87.9
$[NiCl_2(dppe)]$[e]	58.6 (59.1)	4.6 (4.6)	−85.3

[a] All complexes show resonances at δ 2.4 (CH_2CH_2) and 7.1–7.5 (C_6H_5). [b] Calculated values in parentheses. [c] All resonances are singlets. [d] ν(Ni–H) 1950 cm^{-1}, δ −13.1 (qnt, J_{PH} = 5.9 Hz, NiH). For the analogous $[NiH(dppe)_2][HCl_2]$ δ −13.1 (qnt, J_{PH} = 5.9 Hz, NiH) and 13.0 (br, HCl_2^-); ^{2}H NMR spectrum of $[NiD(dppe)_2][DCl_2]$ δ 13.1 (s, NiD) and 10.0 (br, DCl_2^-). [e] When recrystallised from CH_2Cl_2–Et_2O, $[NiCl_2(dppe)] \cdot CH_2Cl_2$ isolated (Found: C, 53.4; H, 4.1. Calc.: C, 52.9; H, 4.2%).

Determination of the HD : D_2 ratios. Analysis of the dihydrogen isotopomer ratios was by use of a MassTorr DX quadrupole analyser mass spectrometer. The reaction studied was that of $[Ni(dppe)_2]$ with anhydrous DCl. The latter was prepared by mixing equimolar concentrations of $SiMe_3Cl$ and MeOD in the solvent of choice. The analyses were performed in an identical fashion to the GC method. The only variation in technique was that a much larger gas sample (10 cm^3) was used. Consequently, repetitive sampling for mass spectral analysis was restricted. Generally a single sample was taken after 2–3 h. The quadrupole analyser separated fragments for H^+, H_2, HD and D_2. The relative ratios of each component were calculated from the peak height, which was normalised to a transducer pressure of 58.6 mbar (5.86 × 10^3 Pa).

Results and Discussion

The reaction of HCl with $[Ni(dppe)_2]$ in either thf or dichloromethane produces stoichiometric amounts of H_2 provided [HCl] ≤ 0.2 mol dm^{-3}. Above this concentration an unidentified decomposition pathway results in decreased dihydrogen yields. However, the course of the reaction is different in the two solvents. The more complicated behaviour is that in dichloromethane but first the simpler reaction in thf will be described.

In thf the products of the reaction are $[NiCl_2(dppe)]$, free dppe and dihydrogen. The identity of the orange crystalline nickel product has been confirmed by X-ray crystallography (Fig. 1); the structure is identical to that reported previously.[9]

The dppe released during the reaction is evident in the ^{31}P-{^{1}H} NMR spectrum of the final reaction solution (δ −155), and is identical to that of authentic dppe.[14] The dihydrogen was identified, and the amount produced quantified, using GC and mass spectrometry.

The reaction occurs in two steps as shown in equation (2).

$$[Ni(dppe)_2] \xrightarrow{HCl} [NiH(dppe)_2]^+ \xrightarrow{HCl} [NiCl_2(dppe)] + dppe + H_2 \quad (2)$$

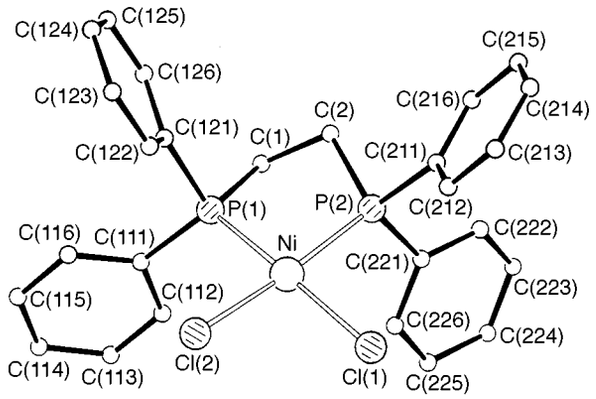

Fig. 1 View of a molecule of $[NiCl_2(dppe)]$. Selected molecular dimensions in the square-planar complex: Ni–Cl(1) 2.2015(8), Ni–Cl(2) 2.1965(8), Ni–P(1) 2.1515(8) and Ni–P(2) 2.1534(7) Å; Cl(1)–Ni–Cl(2) 94.59(3), Cl(1)–Ni–P(1) 171.04(3), Cl(1)–Ni–P(2) 89.47(3), Cl(2)–Ni–P(1) 89.17(3), Cl(2)–Ni–P(2) 175.22(3) and P(1)–Ni–P(2) 87.18(3)°; torsion angle P(1)–C(1)–C(2)–P(2) 49.3(2)°

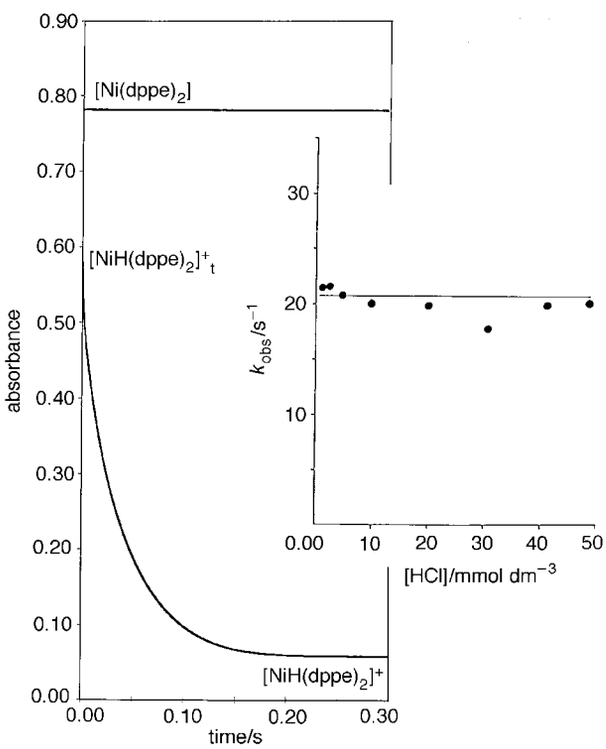

Fig. 2 Stopped-flow absorbance *vs.* time curve (λ = 420 nm) for the reaction between $[Ni(dppe)_2]$ (0.1 mmol dm^{-3}) and HCl (2.5 mmol dm^{-3}) in thf at 25.0 °C. Inset: effect of the concentration of HCl on the value of k_{obs} for the conversion of $[NiH(dppe)_2]^+_t$ into $[NiH(dppe)_2]^+$

Initial formation of $[NiH(dppe)_2]^+$ (complete within 20 s) was followed by release of dihydrogen and formation of $[NiCl_2(dppe)]$ (over 3 h). We will discuss each of these steps separately.

The formation of $[NiH(dppe)_2]^+$

The reaction between $[Ni(dppe)_2]$ and HCl to form $[NiH(dppe)_2]^+$ has been monitored using stopped-flow spectrophotometry. The kinetics show that this simple protonation reaction is unexpectedly complicated. The absorbance *vs.* time curve (Fig. 2) reveals two stages. There is an initial absorbance change which is complete within the dead-time of the apparatus (2 ms). The magnitude of this decrease depends on the concentration of acid. The subsequent formation of $[NiH(dppe)_2]^+$ is associated with an exponential absorbance decrease over the next 0.30 s. Both ^1H and $^{31}P\text{-}\{^1H\}$ NMR spectra confirm that $[NiH(dppe)_2]^+$ is formed at this stage. The kinetics associated with the exponential absorbance decrease shows a first-order dependence on the concentration of $[Ni(dppe)_2]$ {$[Ni(dppe)_2] = (0.25–1.0) \times 10^{-4}$ mol dm^{-3}}, but are independent of the concentration of HCl (Fig. 2). This behaviour is consistent with the mechanism shown in Scheme 1.

Table 2 Spectrophotometric determination of the protonation constant (K_2) of $[Ni(dppe)_2]$ with anhydrous HCl in thf at 25.0 °C (λ = 420 nm), $[Ni(dppe)_2] = 0.1$ mmol dm^{-3}

[HCl]/mmol dm^{-3}	Absorbance	$\{[NiH(dppe)_2]Cl\}_e$[a,b]/ mmol dm^{-3}	K_2[c]/dm^3 mol^{-1}
0.0	0.78		
1.0	0.70	0.012	134
2.5	0.58	0.029	167
5.0	0.45	0.049	188
10.0	0.33	0.066	196
20.0	0.23	0.081	212
30.0	0.21	0.084	172
40.0	0.19	0.087	164
50.0	0.17	0.090	174
100.0	0.10		

[a] $[Ni(dppe)_2]_e = [Ni(dppe)_2]_0 - \{[NiH(dppe)_2]Cl\}_e$. [b] $\varepsilon\{[Ni(dppe)_2]\} = 7.8 \times 10^3$, $\varepsilon\{[NiH(dppe)_2]Cl\} = 1 \times 10^3$ dm^3 mol^{-1} cm^{-1}. [c] $K_2 = \{[NiH(dppe)_2]Cl\}_e/[Ni(dppe)_2]_e[HCl]$.

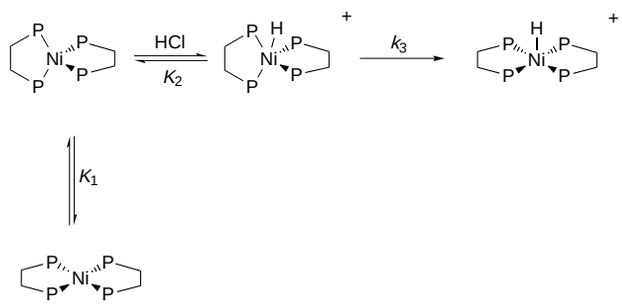

Scheme 1 Mechanism for the reaction between $[Ni(dppe)_2]$ and HCl in thf, to form $[NiH(dppe)_2]^+$

Upon mixing HCl and $[Ni(dppe)_2]$ there is a rapid equilibrium protonation of the complex to form a mixture of $[Ni(dppe)_2]$ and $[NiH(dppe)_2]_t^+$ {'t' designates protonation at a tetrahedral face of $[Ni(dppe)_2]$[15] without changing the gross geometry}. The formation of this mixture corresponds to the initial stopped-flow absorbance decrease. The influence that the concentration of HCl has on the initial absorbance changes has been analysed, as shown in Table 2. This analysis shows that the reaction which is complete within 2 ms, involves the addition of a single proton to $[Ni(dppe)_2]$ ($K_2 = 176 \pm 36$ dm^3 mol^{-1}). Thus, the stoichiometric requirements for the formation of $[NiH(dppe)_2]^+$ have been fulfilled within the dead-time of the stopped-flow apparatus. However, it is clear from inspection of the absorbance *vs.* time curve that the reaction is not complete at this stage. Rather, $[NiH(dppe)_2]_t^+$ undergoes a relatively slow reaction which is independent of the concentration of HCl ($k_3 = 20.7 \pm 3$ s^{-1}). This is consistent with $[NiH(dppe)_2]_t^+$ undergoing an intramolecular rearrangement to the final configuration of $[NiH(dppe)_2]^+$. Although there is no crystal structure of $[NiH(dppe)_2]^+$, the geometry is presumed to be either square-based pyramidal or trigonal bipyramidal. What we are proposing is that protonation of the tetrahedral[15] $[Ni(dppe)_2]$ initially produces $[NiH(dppe)_2]_t^+$, which only relatively slowly rearranges to the final configuration. The kinetics indicate that isomerisation of the tetrahedral $[Ni(dppe)_2]$ to the square-planar form (K_1) followed by protonation of the square-planar isomer is kinetically not so favourable. This may be because protonation of square-planar $[Ni(dppe)_2]$ is slow or, more likely,

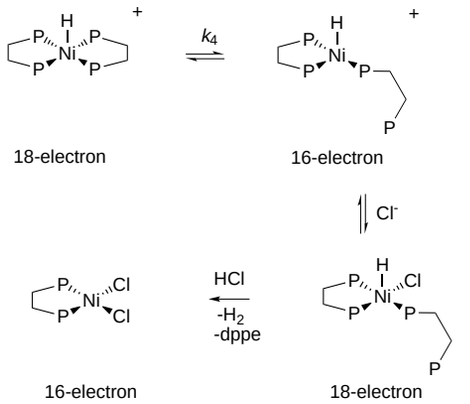

Scheme 2 Proposed mechanism for the reaction between $[NiH(dppe)_2]^+$ and HCl in thf, to form $[NiCl_2(dppe)]$ and H_2

that the bulky phenyl substituents on the dppe ligands make the rate of intramolecular isomerisation slow.

Release of dihydrogen

The kinetics of dihydrogen release from $[NiH(dppe)_2]^+$ have been determined directly by GC. Over the concentration range $10 < [HCl] < 200$ mmol dm^{-3} the rate of dihydrogen production shows a first-order dependence on the concentration of $[NiH(dppe)_2]^+$ $\{[NiH(dppe)_2^+] = 2.5–5.0$ mmol dm$^{-3}\}$ but is independent of the concentration of HCl. The rate law for this process is described by equation (3), with $k_4 = (5.5 \pm 0.7) \times 10^{-4}$ s^{-1}.

$$-d[NiH(dppe)_2^+]/dt = k_4[NiH(dppe)_2^+] \qquad (3)$$

These kinetics are associated with the ultimate formation of dihydrogen, $[NiCl_2(dppe)]$ and free dppe. A mechanism consistent with these observations is shown in Scheme 2. We propose that the rate-limiting step for this stage is phosphine chelate ring opening. This is not unreasonable, since protonation of $[Ni(dppe)_2]$ must decrease the electron density on Ni, thus diminishing the Ni-to-P back bonding and labilising the site to phosphine dissociation.

The simplicity of the kinetics for dihydrogen production from $[NiH(dppe)_2]^+$ means that the rest of the pathway is undefined. However, in line with what has been observed in other protonation reactions,[16] a reasonable sequence of steps is as follows. Dissociation of one phosphorus from $[NiH(dppe)_2]^+$ results in the 16-electron species $[NiH(dppe)(\kappa^1\text{-dppe})]^+$. Binding chloride to this co-ordinatively unsaturated complex increases the electron density at the metal, thus facilitating further protonation and ultimately release of dihydrogen.

Further features of the dihydrogen formation reaction are revealed from studies with DCl. The gaseous products under these conditions were determined by mass spectroscopy as HD (65 ± 5) and D_2 (35 ± 5%), irrespective of the concentration of acid. A fundamental mechanistic point is that we have shown these are the primary products from the reaction. Analysis of the HD and D_2 composition at various times shows that the same proportions of HD and D_2 are produced throughout the course of the reaction. Thus, samples taken at $0.7t_{\frac{1}{2}}$ comprise 63% HD and 37% D_2, at $2.8t_{\frac{1}{2}}$ comprise 63% HD and 37% D_2 and at $8t_{\frac{1}{2}}$ comprise 61% HD and 39% D_2.

A question to be addressed is from where does the hydrogen atom in HD originate? Certainly, this hydrogen atom cannot derive from HCl impurities in the DCl, since the deutero-acid is >90% D labelled. Rather it originates from the phosphine ligand.

The reaction between $[Ni(dppe)_2]$ and DCl has been followed using ^{2}H (D) NMR spectroscopy. The relatively poor solubility of $[NiD(dppe)_2][DCl_2]$ permits isolation of this material {albeit contaminated with the product $[NiCl_2(dppe)]$} during the course of the reaction. The ^{2}H NMR spectrum of this material isolated after *ca.* 1 h shows that deuterium has been incorporated into both the phenyl groups and the CH_2CH_2 groups of dppe (Fig. 3).

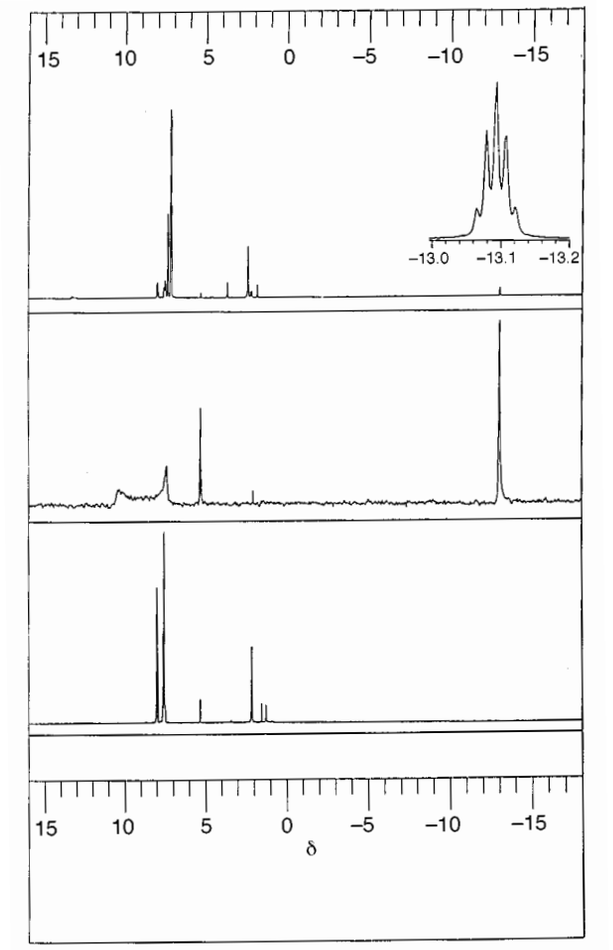

Fig. 3 Top: ^{1}H NMR spectrum of $[NiH(dppe)_2][HCl_2]$ isolated in the reaction between $[Ni(dppe)_2]$ and HCl in thf. Middle: ^{2}H NMR spectrum of $[NiD(dppe)_2][DCl_2]$ isolated in the reaction between $[Ni(dppe)_2]$ and DCl in thf, after *ca.* 1 h. Bottom: ^{1}H NMR spectrum of $[NiCl_2(dppe)]$ isolated at the end of the reaction between $[Ni(dppe)_2]$ and HCl in thf. The ^{2}H NMR spectrum of this material showed no signals. The peak at δ 5.3 in all spectra is due to $CHDCl_2$

One possible pathway for the incorporation of the hydrogen atom into the products involves formal C–H oxidative addition to Ni from a phosphine ligand (Scheme 3).[17] This involves either the phenyl groups or the CH_2CH_2 backbone, but can only occur if the metal is co-ordinatively unsaturated (*i.e.* the 16-electron species containing a monodentate dppe ligand). The relative amounts of HD and D_2 produced by such a pathway would be dictated by the relative rates of this equilibration and the rate of dihydrogen production. However, statistically, it might be expected that this pathway would lead to the predominant formation of HD, with little D_2. An alternative mechanism which could give similar amounts of HD and D_2 is shown in Scheme 4, in which HD is formed directly by the Ni–D group abstracting an H atom from the dppe ligand. Such mechanisms have been proposed before[18] but have, as yet, not been substantiated experimentally.

Changing the dihydrogen isotopomer product

We now turn to the reaction of $[Ni(dppe)_2]$ with HCl in dichloromethane. Detailed product analyses using ^{31}P-{^{1}H} NMR spectroscopy in the acid concentration range $10 < [DCl] < 200$

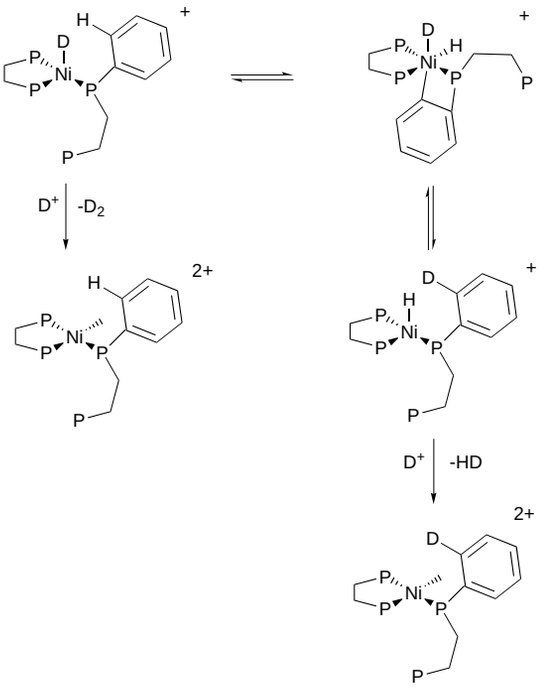

Scheme 3 Suggested pathway by which scrambling of the deutero-ligand and hydrogen atoms on the dppe ligand could occur in $[NiD(dppe)(\kappa^1\text{-dppe})]^+$

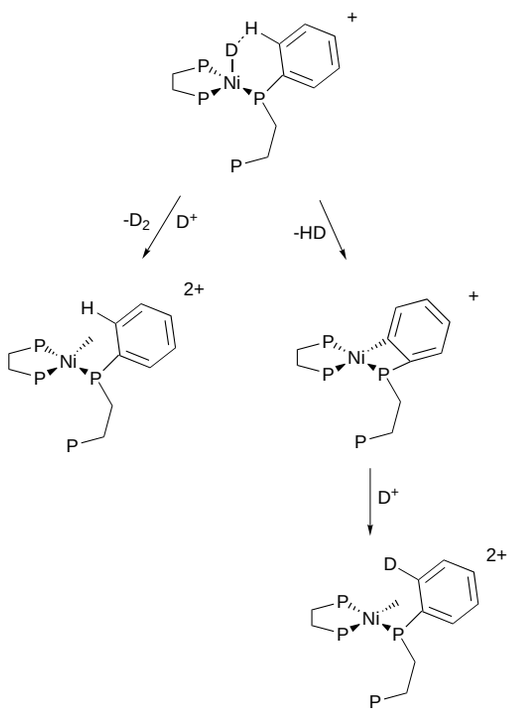

Scheme 4 Suggested alternative pathway to that shown in Scheme 3, for the formation of HD and D_2 involving formal abstraction of an H atom from dppe by the Ni–D group

mmol dm^{-3} show that in this solvent $[Ni(dppe)_2]^{2+}$ is formed at high concentrations of acid, whilst at low concentrations of acid $[NiCl_2(dppe)]$ and free dppe are produced. The formation of $[NiCl_2(dppe)]$ and dppe indicates the same reactivity as in thf, and this is confirmed by the gas mixture produced under these conditions [HD (65 ± 5) and D_2 (35 ± 5%)]. At higher concentrations of DCl the relative proportions of HD and D_2 change (Fig. 4). The complex $[NiCl_2(dppe)]$ has been isolated from the reaction in dichloromethane and characterised by complete crystallographic analysis as the dichloromethane solvate; the structure is the same as that described by Spek

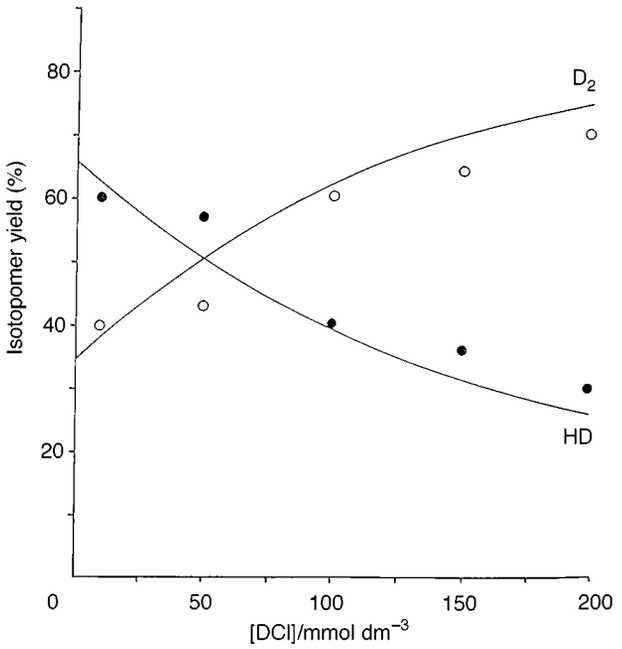

Fig. 4 Effect of the concentration of DCl on the relative amounts of HD and D_2 produced in the reaction with $[Ni(dppe)_2]$ in dichloromethane. The curves drawn are those defined by equations (4) and (5), respectively

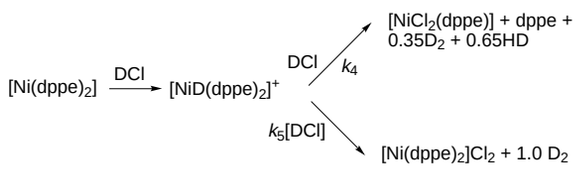

Scheme 5 Pathways for the formation of HD and D_2 in the reaction between $[Ni(dppe)_2]$ and DCl in dichloromethane

et al.[19] {Busby *et al.*[9] compared the conformations in the complexes in solvated and unsolvated crystals, noting that the principal difference is in the orientation of the phenyl rings; an axis of pseudo-symmetry through the $[NiCl_2(dppe)]$ molecule in the solvated crystal is not present in the unsolvated complex.}

In dichloromethane, kinetic studies show that, at low concentrations of acid, the rate of dihydrogen production is essentially the same as that observed in thf. However, at higher acid concentrations an additional pathway forming $[Ni(dppe)_2]^{2+}$ is kinetically significant.

Analysis of the HD/D_2 product distribution allows the kinetics for the reaction at high concentrations of acid to be determined. The curves drawn in Fig. 4 are the best fit to the product distribution data, and are defined by equations (4) and (5). This

$$\text{Fraction of HD} = \frac{0.65}{1 + 8.1\,[\text{DCl}]} \quad (4)$$

$$\text{Fraction of } D_2 = \frac{0.35 + 8.1\,[\text{DCl}]}{1 + 8.1\,[\text{DCl}]} \quad (5)$$

product distribution is consistent with the reactions shown in Scheme 5. The top route is that already described in thf, involving rate-limiting dissociation of dppe. The bottom pathway involves attack of DCl on $[NiD(dppe)_2]^+$ in a reaction which we propose exhibits a first-order dependence on the concentration of acid (k_5).

The kinetics for these pathways predict the HD/D_2 product distribution[20] as follows: HD is formed only in the top pathway of Scheme 5 and its amount is described by equation (6); how-

ever, D_2 is formed by both routes and the amount of this isotopomer is defined by equation (7).

$$\text{Amount of HD} \propto 0.65k_4[\text{NiD(dppe)}_2]^+ \quad (6)$$

$$\text{Amount of } D_2 \propto (1.0k_5[\text{DCl}] + 0.35k_4)[\text{NiD(dppe)}_2]^+ \quad (7)$$

We can use these two equations to predict the yields of HD and D_2 [equations (8) and (9) respectively].

$$\frac{[\text{HD}]}{[\text{D}_2] + [\text{HD}]} = \frac{0.65}{1 + (k_5/k_4)[\text{DCl}]} \quad (8)$$

$$\frac{[\text{D}_2]}{[\text{D}_2] + [\text{HD}]} = \frac{0.35 + (k_5/k_4)[\text{DCl}]}{1 + (k_5/k_4)[\text{DCl}]} \quad (9)$$

Comparison of equations (8) or (9) with (4) or (5) respectively shows that $k_5/k_4 = 8.1$. Since $k_4 = (5.5 \pm 0.7) \times 10^{-4}$ s^{-1} we can estimate $k_5 = 4.5 \times 10^{-3}$ dm^3 mol^{-1} s^{-1}.

For the k_5 pathway the first-order dependence on the concentration of DCl indicated by this analysis is consistent with a simple mechanism involving direct deuteriation of $[\text{NiD(dppe)}_2]^+$ at Ni (or the deutero-ligand). This produces $[\text{NiD}_2\text{(dppe)}_2]^{2+}$ {or $[\text{Ni(D}_2\text{)(dppe)}_2]^{2+}$} which subsequently releases D_2. Our simulation of the HD/D_2 product distribution is based on the assumption that the k_5 pathway gives only D_2. This is reasonable since, in this pathway, the formation and release of D_2 always involves an 18-electron nickel species. It seems unlikely that during this reaction there would be facile oxidative addition to Ni of a C–H group from the dppe ligand.

Comparisons with other systems

In this paper we have shown that the mechanism for the formation of dihydrogen isotopomers, in the reaction between $[\text{Ni(dppe)}_2]$ and DCl, depends on the solvent and the concentration of acid. Most important, we have shown that by varying the concentration of DCl different mixtures of HD and D_2 can be produced.

Controlling the products of a reaction by varying the concentration of acid is a feature which has been exploited in the reactions of unsaturated hydrocarbons bound to electron-rich sites. For example, the reaction of HCl with *trans*-$[\text{Mo}(\eta^2\text{-C}_2\text{H}_4)_2\text{(dppe)}_2]$ [21] produces 1 mol equivalent of ethane and 1 mol equivalent of ethylene at low concentrations of acid. At high concentrations of acid 2 mol equivalents of ethylene are produced. This is a consequence of competitive protonation reactions at the co-ordinated ethylene and Mo. The more rapid pathway at low concentrations of acid involves protonation of a co-ordinated ethylene, which ultimately produces ethane. The other ethylene ligand dissociates from Mo. Protonation of Mo labilises both ethylene ligands to dissociation; however, it is a slow reaction and only dominates at high concentrations of acid.

A similar sequence of reactions also results in the selective formation of propene and propyne from the reaction of HCl with *trans*-$[\text{MH}(\eta^3\text{-C}_3\text{H}_5)\text{(dppe)}_2]$ (M = Mo or W).[22] Again, it is a facile protonation of the hydrocarbon ligand which dominates the kinetics at low concentrations of acid and results in the formation of propene. At high concentrations of acid diprotonation of Mo becomes kinetically significant, and ultimately results in the formation of propyne.

The points which are common to these studies on hydrocarbon systems are: (i) proton attack can occur at either the ligand or the metal and (ii) the kinetics for the two product-forming pathways exhibit different dependences on the concentration of acid. It is because of these features that the products of the reactions can be controlled by varying the concentration of acid.

This strategy is not applicable for metal hydrides because

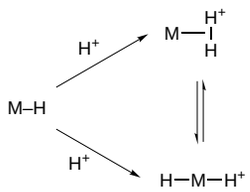

Scheme 6

protonation of the metal gives a dihydride, whilst protonation of the hydride ligand gives a dihydrogen species (Scheme 6). These species invariably equilibrate rapidly.[23] Unless there is a way of suppressing this equilibration the two pathways would give the same mixture of dihydrogen isotopomers.

The work described herein reveals another way by which varying the concentration of acid can result in different products. The initial formation of $[\text{NiD(dppe)}_2]^+$ labilises a dppe ligand to dissociation. This generates a vacant site in the co-ordination sphere of the metal which allows scrambling of the deuterium on Ni with hydrogen atoms on the dppe ligand and results in the ultimate production of HD. At higher concentrations of DCl, deuteriation of $[\text{NiD(dppe)}_2]^+$ becomes faster than dissociation of dppe and consequently results in the production of D_2.

There is only one other mechanistic study on dihydrogen production from a nickel complex of which we are aware [5] [equation (10)]. The mechanism of this reaction is quite different

$$2[\text{Ni}\{\text{HN(CH}_2\text{CH}_2\text{SCH}_2\text{CH}_2\text{PPh}_2)_2\}]^+ + 2\text{HCl} \xrightarrow{\text{Me}_2\text{NCHO}} 2[\text{Ni}\{\text{HN(CH}_2\text{CH}_2\text{SCH}_2\text{CH}_2\text{PPh}_2)_2\}]^{2+} + 2\text{Cl}^- + \text{H}_2 \quad (10)$$

from that described in this paper, but some common features are evident. Thus, initial protonation of the Ni gives a hydrido-intermediate, $[\text{NiH}\{\text{HN(CH}_2\text{CH}_2\text{SCH}_2\text{CH}_2\text{PPh}_2)_2\}]^{2+}$. Subsequent coupling of hydride ligands between two such species ultimately produces dihydrogen. Presumably, a dihydrogen-forming pathway, involving direct protonation of the nickel(III) species $[\text{NiH}\{\text{HN(CH}_2\text{CH}_2\text{SCH}_2\text{CH}_2\text{PPh}_2)_2\}]^{2+}$ is much slower. This is consistent with our observations on the nickel(II) species $[\text{NiH(dppe)}_2]^+$. Protonation of $[\text{NiH(dppe)}_2]^+$ only occurs in dichloromethane at high concentrations of acid. At low concentrations of acid alternative, more facile, dihydrogen-forming pathways are available which involve changes to the co-ordination sphere of the Ni.

Acknowledgements

We thank the BBSRC for supporting this work and funding the equipment (Equipment Grant Number EQP05815).

References

1 V. Koelle, *New J. Chem.*, 1992, **16**, 157 and refs. therein.
2 A. C. Albeniz, D. M. Heinekey and R. H. Crabtree, *Inorg. Chem.*, 1991, **30**, 3632 and refs. therein.
3 R. A. Henderson, S. K. Ibrahim, K. E. Oglieve and C. J. Pickett, *J. Chem. Soc., Chem. Commun.*, 1995, 1571 and refs. therein.
4 J. Chatt, F. A. Hart and H. R. Watson, *J. Chem. Soc.*, 1962, 2532.
5 T. L. James, L. Cai, M. C. Muetterties and R. H. Holm, *Inorg. Chem.*, 1996, 35, 4148.
6 A. F. Williams, *Acta Crystallogr., Sect. C*, 1989, **45**, 1002 and refs. therein.
7 G. M. Sheldrick, SHELX 76, Program for crystal structure determination, University of Cambridge, 1976.
8 G. M. Sheldrick, SHELXL 93, Program for crystal structure refinement, University of Göttingen, 1993.
9 R. Busby, M. B. Hursthouse, P. S. Jarrett, C. W. Lehmann, K. M. A. Malik and C. Phillips, *J. Chem. Soc., Dalton Trans.*, 1993, 3767.
10 *International Tables for X-Ray Crystallography*, Kynoch Press, Birmingham, 1974, vol. 4, pp. 99 and 149.
11 S. N. Anderson, R. L. Richards and D. L. Hughes, *J. Chem. Soc., Dalton Trans.*, 1986, 245.

12 R. A. Henderson, *J. Chem. Soc.*, *Dalton Trans.*, 1982, 917.
13 R. G. Wilkins, *Kinetics and Mechanism of Reactions of Transition Metal Complexes*, 2nd edn., VCH, Weinheim, 1991, ch. 1.
14 R. A. Henderson and K. E. Oglieve, *J. Chem. Soc.*, *Dalton Trans.*, 1994, 767.
15 P. M. Boorman, G. K. W. Freeman and M. Parvez, *Polyhedron*, 1992, **11**, 765.
16 D. J. Evans, R. A. Henderson and B. E. Smith, *Bioinorganic Catalysis*, ed. J. Reedijk, Marcel Dekker, New York, 1993, p. 89 and refs. therein.
17 L. N. Lewis and J. F. Smith, *J. Am. Chem. Soc.*, 1986, **108**, 2728.
18 A. C. Albéniz, G. Schulte and R. H. Crabtree, *Organometallics*, 1992, **11**, 242 and refs. therein.
19 A. L. Spek, B. P. van Eijck, R. J. F. Jans and G. van Koten, *Acta Crystallogr.*, *Sect. C*, 1987, **43**, 1878.
20 J. H. Espenson, *Chemical Kinetics and Reaction Mechanisms*, McGraw Hill, New York, 1981, p. 55.
21 R. A. Henderson and K. E. Oglieve, *J. Chem. Soc.*, *Dalton Trans.*, 1991, 3295 and refs. therein.
22 R. A. Henderson, D. L. Hughes, C. J. Macdonald and K. E. Oglieve, *Inorg. Chim. Acta*, 1997, **259**, 107 and refs. therein.
23 P. G. Jessop and R. H. Morris, *Coord. Chem. Rev.*, 1992, 155 and refs. therein.

Received 8*th October* 1997; *Paper* 7/07275I